Two-Frequency Motion to Chaos with Fractal Dimension $d > 3$

Hie-Tae Moon

Department of Physics, Korea Advanced Institute of Science and Technology, Daeduk Science-town 305-701, Korea

(Received 14 April 1997)

A direct transition from two-frequency motion to chaos with a fractal dimension of $d > 3$ is illustrated. While frequency locking between the two frequencies is a characteristic onset feature when the chaos involved has a lower dimension of $d < 3$, no such feature is found in the present case. [S0031-9007(97)03597-7]

PACS numbers: 05.45.+b

One of the well-known routes to chaos is the route to chaos from a two-frequency quasiperiodic motion [1–5]. Evidence of this particular route to chaos was first known in late 1970s [1,2]. Still, our understanding of the transition appears quite limited.

A common method of displaying the dynamics is through a Poincaré section, which is simply a slice of a complicated trajectory across, for example, the center of the trajectorial motion. On the Poincaré section, a circular ring refers to a torus representing a two-frequency quasiperiodic motion in the continuous flow. Often, one studies an iterated two-dimensional (2D) mapping as a model of the Poincaré section of a continuous 3D flow. The characteristic onset feature to chaos found in such a study [1] is the development of wrinkles or corrugations on the ring, preceded by frequency locking, signaling that the folding [6] on the torus is taking place, leading directly to a strange attractor [7]. The theoretical ground of our understanding for the existence of frequency locking at the onset was thus primarily geometrical. The same manner of the transition was identified in the continuous 3D flows described by the forced Van der Pol's equations [8]. A more formal mathematical approach for this transition has been made in terms of the mapping of a circle onto itself [8–11].

We note, however, that information based on 2D maps is meant to be applicable to the chaos with a low dimension of $d < 3$. A further clarification of this type of transition in the case of higher dimensional chaos is needed. In this regard, we notice that while some experimental observations [2,12] show the characteristic onset features as predicted by the 2D models, certain experiments find a direct thickening, or dispersion, of a torus without any evidence of frequency locking [12,13]. It was then speculated that such a chaotic regime might correspond to a strange attractor with a dimension of greater than three [14]. This conjecture remains unsettled. Along with this conjecture exists a rather intriguing question; namely, whether the chaos with a higher dimension of $d > 3$ has indeed a threshold R_2 directly from the two-frequency motion ($d = 2$), or through a threshold R_3 of quasiperiodicity with three frequencies ($d = 3$) [7,15] which could be very close to, or even right at, R_2 [3–5]. Here, we address this issue.

As a natural extension, one may attempt to consider an iterated 3D mapping, simulating the Poincaré map of a continuous 4D flow. An existing study [16] of such a model has shown that a torus can also lose its stability through a cascade of period doublings, and that a torus, after a few times of period doubling, is more likely to lose its stability by developing the folding around itself preceded by a frequency locking, as predicted in the 2D models. In general, the dynamics of a 3D map itself are already very complicated, so setting up an informative 3D mapping model turns out by no means to be a simple matter. As an alternative, one might first consider a continuous 4D flow, and then attempt to construct the corresponding 3D Poincaré maps directly from the flow, hoping for general information on the transition. Here, we take the latter approach and consider the following phenomenological model of a 4D continuous flow [17],

$$\begin{aligned} \dot{a}_1 &= \epsilon a_1 + (i - \epsilon)\,(|a_1|^2 a_1 + a_1|a_2|^2 + \tfrac{1}{2}a_1^* a_2^2)\,, \\ \dot{a}_2 &= \epsilon a_2 - q^2(i + \epsilon)a_2 + (i - \epsilon) \\ &\quad \times (a_1^2 a_2^* + 2|a_1|^2 a_2 + \tfrac{3}{4}|a_2|^2 a_2)\,, \end{aligned} \tag{1}$$

where $\dot{a}_1, \dot{a}_2$ denote, respectively, the time derivative of the complex variables $a_1(t), a_2(t)$, ϵ is a smallness parameter related to energy input and dissipation rate set at 0.05, and q is a control parameter. The flow possesses a periodic solution with frequency $\omega = 1$

$$a_1(t) = e^{it}. \tag{2}$$

A slight perturbation to this periodic solution as

$$a_1(t = 0) = 1, \qquad a_2(t = 0) = \delta, \qquad \delta \ll 1\,, \tag{3}$$

at $q = 0.98$, leads to a two-frequency motion with two irrational frequencies [Fig. 1(a)]. For a slightly lower $q = 0.97$, this two-frequency motion turns itself directly to chaos characterized by a broadband spectrum [Fig. 1(b)].

To see the characteristic feature of this chaotic flow, we measured the maxima of the time signal $b(t) = |a_2(t)|$. Denoting the ith maximum of $b(t)$ as M_i, we also measured the period τ_i between successive maxima M_i and M_{i+1}. Plotting τ_{i+1} as a function of τ_i for all $i = 1, 2, 3, \ldots$, we obtain a noninvertible one-dimensional map

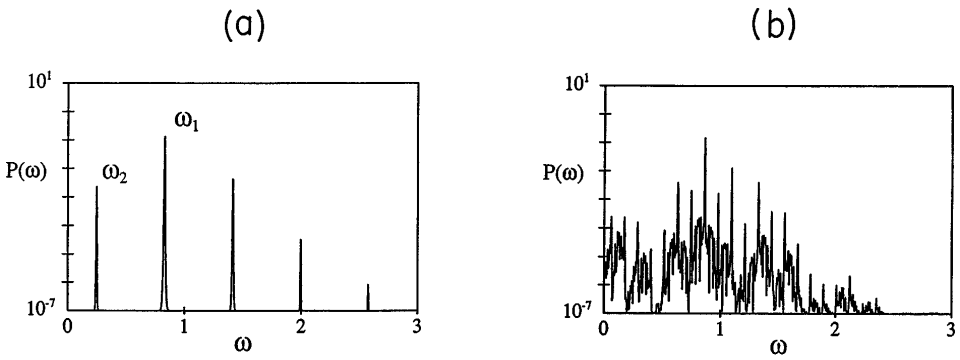

FIG. 1. Power spectrum of (a) the two-frequency motion at $q = 0.98$; ω_1, ω_2 are the two independent frequencies, and the others are the linear sums of these two, and (b) the chaotic motion at $q\ (= 0.97) < 0.98$.

[Fig. 2], which indicates that the flow is now in a strange attractor.

To understand the detailed manner of the transition between the two flows, we need to investigate their geometries. Since the trajectory travels in the 4D state space spanned by $X = \mathrm{Re}[a_1]$, $W = \mathrm{Im}[a_1]$, $Y = \mathrm{Re}[a_2]$, and $Z = \mathrm{Im}[a_2]$, we may take the trajectory's 3D Poincaré map as follows. Whenever the trajectory passes through the plane $W = 0$ with a direction $\dot{W} > 0$, we mark the other three coordinates (X, Y, Z) of the piercing point. The nth point (X_n, Y_n, Z_n) is then uniquely mapped into the next point $(X_{n+1}, Y_{n+1}, Z_{n+1})$ under such a procedure, which defines a 3D Poincaré map of the trajectory. The marked points now form a discrete trajectory in the 3D XYZ space, where we can now visualize the trajectorial motion.

The results are displayed in Fig. 3, where the two-frequency state forms a ring, i.e., a torus [Fig. 3(a)], while the chaotic state gives a more complicated structure, the strange attractor [Fig. 3(b)].

A detailed analysis of the data obtained from a set of initial conditions scattered over the geometric structures leads to the conclusion that the ring is in fact formed by an interplay of three neighboring unstable fixed points.

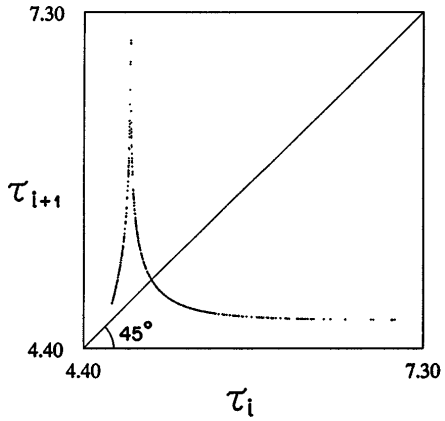

FIG. 2. A noninvertible 1D map produced by the chaotic flow of Fig. 1(b). This provides evidence that the motion is in a strange attractor.

Figure 3(a) shows these three unstable fixed points, denoted by α, β_L, and β_R, together with the complete structures of their stable and unstable manifolds. Among the three, α at the center corresponds to the original periodic state $a_1(t) = e^{it}$ that was perturbed. Once the locations of the three unstable fixed points are identified, it is then straightforward to analyze the local flows around each of them numerically.

Results of the linear stability analysis around each fixed point show that α has three positive real eigenvalues. The first one is greater than 1 (1 being the stability criterion), corresponding to the unstable manifolds denoted by s_α and s'_α, while the other two are less than 1, corresponding to the stable planar manifold denoted by A. The results also show that β_L and β_R, on the other hand, have a complex conjugate pair with an amplitude greater than 1, corresponding to the spirally outgoing separatrices s_β and s'_β along the unstable planar manifolds B_L and B_R, and have another eigenvalue, which is positive real but less than 1, defining stable manifolds indicated by the arrows directed toward the planes B_L and B_R.

From local information around each fixed point and from the continuity as well as the uniqueness of a trajectory, we can construct the global geometry of the stable and unstable manifolds of the three unstable fixed points. The complete geometry for the ring presented in Fig. 3(a) has been constructed in this way. The ring is stable between s_α and the heteroclinic orbit s'_β and between s'_α and s_β, while s_α, s'_α are asymptotically approaching the torus. Under this geometry, we can see that the entire space becomes the basin of attraction for the torus: All the trajectories in the space except those exactly on the heteroclinic orbits s_β or s'_β are eventually attracted to the torus by being guided by s_α or s'_α.

It turns out that this global geometry for the torus in fact gives all the answers to the questions raised at the beginning. Notice that the geometry of the strange attractor displayed in Fig. 3(b) is nothing but the unstable manifolds s_α and s'_α of α. A detailed comparison of Figs. 3(a) and 3(b) indicates that the merging of the manifold s_α with the heteroclinic orbit s'_β and the merging

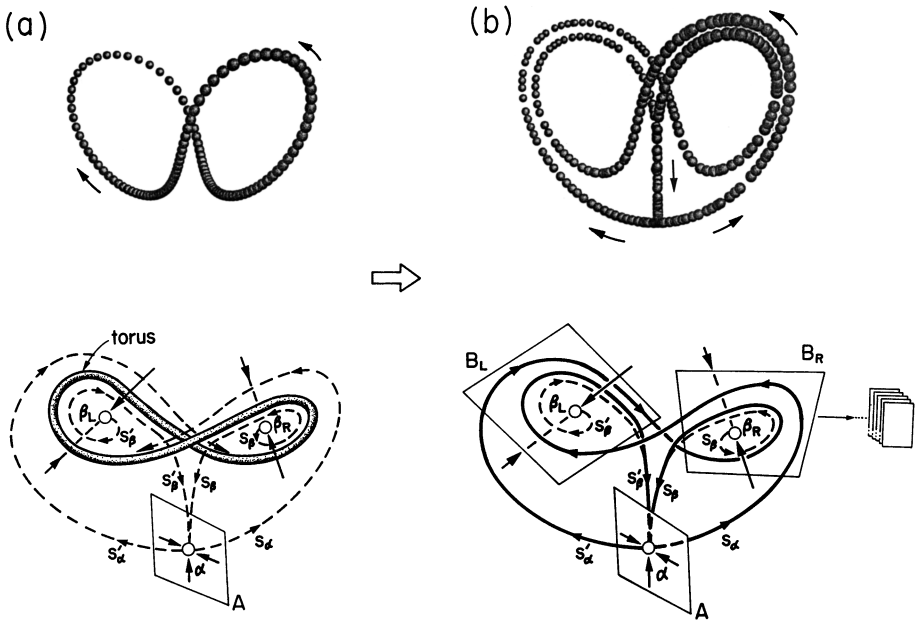

FIG. 3. Illustration of the global geometries in the 3D Poincaré map. (a) Upper plot: The torus of the two-frequency motion. Lower plot: The global geometry of the torus. The torus is formed by an interplay of three unstable fixed points α, β_L, and β_R. s_α, s'_α are the unstable manifolds of α, and the plane A is the stable manifold of α. The planes B_L and B_R are the unstable manifolds of, respectively, β_L and β_R. s_β and s'_β are the heteroclinic orbits connecting β_L and β_R to α. (b) Upper plot: The strange attractor. Lower plot: Notice that the strange attractor is nothing but the unstable manifolds of α. The merging of s_α and s'_α with the heteroclinic orbits s'_β and s_β, respectively, causes destruction of the torus.

of s'_α with s_β finally lead to the "destruction" of the torus. As it is, the torus collapses completely while the continuous unstable manifolds of α appear. Apparently, there are no such features of wrinklings or corrugations of the torus preceded by frequency locking, characteristic of the torus breakup in the 2D models [1,8]. The unstable manifolds are largely retracing the previous torus site again and again, making it thickened or dispersed. In addition, it is clear that the transition is not effected by the form of a third frequency. Consequently, the detailed global geometries illustrated here provide a geometrical explanation for the *direct* transition from a torus ($d = 2$) to a strange attractor with a higher fractal dimension of $d > 3$ (to be argued next).

Since the only passage to α is already occupied by the heteroclinic orbits s_β and s'_β, the outgoing manifolds of α cannot close themselves at α. The broadband spectrum in Fig. 1(b) is an indication that the unstable manifold of α does not close itself. Another piece of evidence is, of course, the more technical 1D noninvertible return map of Fig. 2. If the unstable manifold is not closed, then it has to make a set of an infinite number of closely located circular orbits that do not touch one another, thanks to the uniqueness of a trajectory. We may then view each circular orbit as lying on a separate surface. Thus, the unstable manifold is effectively defining a set of infinitely many and arbitrarily closely located *fractal* planes, as indicated by the icon in Fig. 3(b). This set of an infinite number of fractal planes has a noninteger dimension in between $d = 2$, the dimension of a surface, and $d = 3$, the dimension of a volume.

One may notice that the geometry here is almost identical to that of the well-known Lorenz attractor [18], which has a fractal dimension of $2 < d < 3$. A clear difference, however, is that while the Lorenz attractor lives in continuous 3D space, the current structure exists in a 3D Poincaré map. In a Poincaré map, a ring ($d = 1$) represents a torus ($d = 2$) living in a continuous flow. Likewise, a strange attractor with a fractal dimension of $2 < d < 3$ in a Poincaré map represents a strange attractor with a fractal dimension of $3 < d < 4$ in a continuous flow. Thus, we are led to the conclusion that the two-frequency motion ($d = 2$) shown in Fig. 1(a) was destroyed directly to chaos with a fractal dimension of $3 < d < 4$, not in the form of a third frequency ($d = 3$).

Presently, not many details of the geometrical structures of strange attractors in four dimensions are known in comparison to those in three dimensions. This may be due in part to the serious visualization problem encountered in four dimensions. The structure we found here is like adding the dimension by one to each building block of the Lorenz attractor; namely, the three unstable fixed points in the Lorenz attractor are replaced by three unstable periodic orbits.

Finally, how might it have looked if the present transition had been measured experimentally where the Poincaré map might have been projected on a plane? Figure 4 shows a schematic drawing of a 2D Poincaré section (an

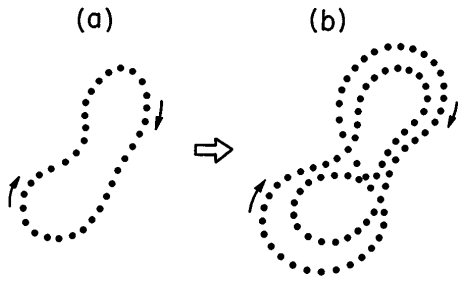

FIG. 4. A schematic drawing of the 2D Poincaré section (upper view of the 3D Poincaré map). It shows a direct thickening of the torus at the onset, without any corrugations preceded by frequency locking.

upper view of the 3D Poincaré map) of the transition, where one observes a direct thickening of the torus at the onset in the same manner as it was observed in the existing experiments [12,13].

To summarize, we have illustrated geometrically how a two-frequency motion ($d = 2$) may lose its stability directly to chaos with a fractal dimension of $d > 3$. Details of the strange attractor are also illustrated. Unlike the transition involving lower dimensional chaos ($d < 3$), where frequency locking is a characteristic onset feature, this transition does not go through the frequency-locking process at the onset.

The author wishes to thank U. Fano for many cheerful discussions. Preparation of this report was supported by the Korea Science and Engineering Foundation.

[1] J. Curry and J. A. Yorke, in *Springer Notes in Mathematics* (Springer-Verlag, Berlin, 1977), Vol. 668, p. 48.
[2] J. P. Gollub and S. V. Benson, in *Pattern Formation and Pattern Recognition*, edited by H. Haken (Springer-Verlag, Berlin, 1979), p. 74.
[3] J. P. Gollub and S. V. Benson, J. Fluid. Mech. **100**, 449 (1980).
[4] See, for example, J.-P. Eckmann, Rev. Mod. Phys. **53**, 643 (1981).
[5] See, for example, H. L. Swinney, Physica (Amsterdam) **7D**, 3 (1983).
[6] S. Smale, Bull. Am. Math. Soc. **73**, 747 (1967).
[7] D. Ruelle and T. Takens, Commun. Math. Phys. **20**, 167 (1971).
[8] P. Coullet, C. Tresser, and A. Arnéodo, Phys. Lett. **77A**, 327 (1980).
[9] D. G. Aronson, M. A. Chory, G. R. Hill, and R. P. MaGehee, Commun. Math. Phys. **83**, 303 (1982).
[10] D. Rand, S. Ostlund, J. Sethna, and E. Siggia, Phys. Rev. Lett. **49**, 132 (1982).
[11] M. J. Feigenbaum, L. P. Kadanoff, and S. J. Shenker, Physica (Amsterdam) **5D**, 370 (1982).
[12] M. Dubois and P. Berge, J. Phys. (Paris) **42**, 167 (1981).
[13] D. Farmer, J. Hart, and P. Weidman, Phys. Lett. **91A**, 22 (1982).
[14] See, for example, P. Berge, Y. Pomeau, and C. Vidal, *Order Within Chaos* (Wiley, New York, 1984), p. 168.
[15] S. Newhouse, D. Ruelle, and T. Takens, Commun. Math. Phys. **64**, 35 (1978).
[16] A. Arnéodo, P. Coullet, and E. Spiegel, Phys. Lett. **94A**, 1 (1983).
[17] This model is the two modes truncation of the complex coefficient Ginzburg-Landau equation.
[18] E. N. Lorenz, J. Atmos. Sci. **20**, 130 (1963).